AIAA JOURNAL
Vol. 33, No. 9, September 1995

Influence of Pressure Waves on the Initial Development of an Explosion Kernel

A. C. McIntosh*
University of Leeds, Leeds LS2 9JT, England, United Kingdom

The paper discusses the role of pressure waves in the propagation of deflagrations immediately after ignition. The effect of one-dimensional pressure interactions upon the mass burning rate of a planar flame is first of all discussed, whereby it is shown that there can be a large transient effect on the mass flux through the flame at different locations in the reaction zone. The paper then goes on to discuss two-dimensional effects, in particular the baroclinic production of vorticity leading to the eventual breakup of a laminar flame into a series of turbulent flamelets.

I. Explosions and Pressure Waves—General Introduction

THE need to understand the role of pressure waves in explosion theory has been well documented in recent disasters. The blast wave from unconfined explosions can be very severe and soon turn into a shock,[1] and when turning to partially confined explosions, the role of pressure waves is increased further due to the presence of obstacles. This is borne out for instance by the large overpressures recorded in accidents such as that at Flixborough, United Kingdom, on June 1, 1974.

Flixborough of course is generally recognized as a turning point in social awareness of the hazards involved in some parts of the chemical industry. It was also the beginning of a drive to understand more clearly the science of explosion propagation as it related to the safe operation of a potentially hazardous plant. The very high rate of pressure rise at Flixborough of between 8.2 and 17.6 bar s^{-1} may have been due to the chemical piping, not only causing turbulence and increases in the flame speed, but also encouraging reflections of the initial pressure waves back into the oncoming deflagration front.

The evidence from the public inquiry into another United Kingdom incident—the Piper Alpha disaster of July 6, 1988 (see Sec. 5.95 of Ref. 2)—suggests overpressures for the initial explosion of approximately 0.2–0.4 bar but with not as large a rate of pressure rise. It was the subsequent uncontrolled fire that caused the greater loss of life in this case. Nevertheless, the comparison of these two incidents alone illustrates that very different phenomena can be involved in what outwardly may appear similar scenarios. The explosions in various incidents cannot usually be traced back to a common single cause, but there have been sufficient incidents similar to Flixborough that indicate that very fast initial accelerations of the burning velocity are common.

One further incident is sufficient to show the damage that can be done by the initial explosion. On June 6, 1989, approximately 600 people were killed when two trains of the Trans Siberian Railway were blown off the rails due to the explosion of a gas cloud leaking from a nearby pipeline. Trees within a radius of nearly 2 miles were flattened, and windows 7 miles away were smashed. Further details have not been forthcoming but the rate of initial pressure rise was evidently very large. It is the initial stages of this process that are all important. If the mass burning rate is abnormally increased by turbulence or pressure wave interactions, then the flame speed will increase markedly, adding greatly to the strength of the precursor blast wave.

Received Nov. 1, 1993; presented as Paper 94-0104 at the AIAA 32nd Aerospace Sciences Meeting, Reno, NV, Jan. 10–13, 1994; revision received Nov. 21, 1994; accepted for publication Nov. 21, 1994.

*Senior Lecturer, Department of Fuel and Energy. Member AIAA.

Thus, in summary the thinking behind this work is as follows. Undoubtedly one of the effects of obstacles is to increase the turbulence and consequently the burning rate of any explosive mixture in their vicinity. A considerable amount of research has concentrated effort in this direction, including, in particular, experimental work by Lee,[3] Lee and Moen,[4] and Moen et al.[5] Much of the initial pioneering work in understanding flame acceleration was undertaken by Oppenheim, who has more recently considered the self-similar development of blast waves emanating from explosions.[6,7] But another phenomenon little understood is the effect of reflected pressure waves passing through the zone of intense reaction (see Fig. 1). It is this aspect of explosions that this paper seeks to address, both analytically and numerically.

II. Time and Length Scales (Refer to Fig. 2)

The two important and fundamental ratios[8,9] occurring are

$$\tau \equiv \frac{\text{diffusion time}}{\text{acoustic time}}$$

$$N \equiv \frac{\text{characteristic length of pressure disturbance}}{\text{diffusion length}}$$

If M is taken to be the Mach number of flame propagation, i.e.,

$$M \equiv u'_{01}/a'_{01}$$

where u'_{01} is the initial burning velocity and a'_{01} the sound speed, then it follows that

$$\tau = 1/NM$$

To concentrate on the major effects of time and length scale effects, we consider the flame to be characterized by one overall Arrhenius reaction with a nondimensional activation energy θ defined as

$$\theta \equiv E'_A/R'T'_b$$

The actual activation energy $E_{A'}$ is nondimensionalized using the burnt temperature $T_{b'}$. The inverse θ^{-1} then measures the thickness of the region of intense chemical activity (the reaction zone).

There are three distinct cases of pressure/premixed flame interaction:

1) $N = 1/M$: $\tau = 1$: Pressure gradients are not important in the combustion region; the inner reaction zone is not affected by the pressure field. The effect of the pressure disturbances is predominantly in the outer combustion zones (preheat and equilibrium) where the equations and jump conditions govern the connection between the mass flux and pressure transients.

2) $N = 1/(\theta^2 M)$: $\tau = \theta^2$: Pressure gradients are still not felt in the combustion region; however, the fast time scale now causes the pressure changes to affect the inner reaction zone. A different

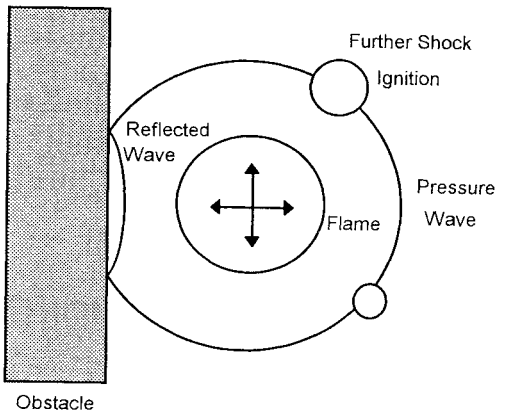

Fig. 1 Pressure interaction effects during early stages of ignition.

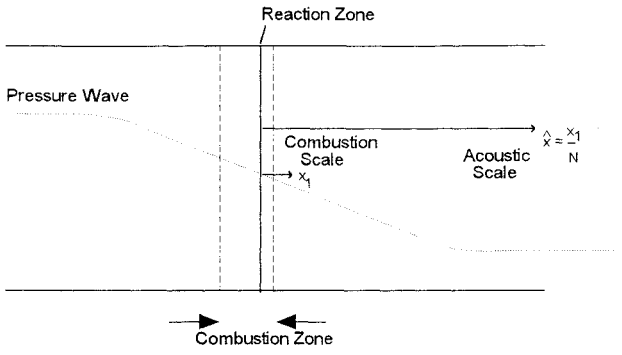

Fig. 2 Typical length and time-scales for pressure interactions with flames.

equation to that in the preceding paragraph now determines the connection between the mass flux and the pressure changes.

3) $N = 1: \tau = 1/M$: Pressure gradients are now important in the combustion region, which contains the full effect of any pressure wave passing through. Nonconstant wave speed with nonlinearities exist for large amplitude disturbances; the pressure changes are of an ultrashort length scale.

III. One-Dimensional Interactions

A. Acoustic Coupling

In some earlier papers[10–12] very low amplitude acoustic coupling of flames was investigated where the disturbances were of medium wavelength ($\tau \approx 1: N \approx M^{-1}$). The assumption of low amplitude (δ) of the disturbance [$\delta \approx \mathcal{O}(M)$] meant that the only coupling was through the velocity perturbation. It was then found that the velocity perturbation was only affected by the flame when heat loss came into effect. In the absence of heat loss, such low-level acoustics simply regarded the flame as a contact discontinuity swept along with the small unsteady acoustic waves. Under the assumption of small amplitude [$\delta \approx \mathcal{O}(M)$], there was no coupling of pressure changes with the temperature disturbances at the flame. However, this situation changes when δ is raised to a value near θ^{-1}, when such a coupling can take place. Assuming the perturbation amplitude δ to be near θ^{-1}, van Harten et al.[13] considered acoustic coupling of flames with $\tau \ll 1$ ($N \gg M^{-1}$: very long wavelengths) and $\tau \approx 1$ ($N \approx M^{-1}$: medium wavelengths). Density effects were included in the first case but not in the second. In a later paper[9] the restriction of constant density is lifted (still with the amplitude $\delta \approx \theta^{-1}$) and replaced with the more realistic assumption that density ρ' times thermal conductivity λ' is constant.

The $N \approx M^{-1}$ ($\tau \approx 1$) length scale (case 1) of pressure disturbance is typical of industrial and domestic boiler noise and noise associated with burners. It is also the appropriate length scale to describe flame buzz in engines (≈100–600 HZ). The time taken by the pressure wave to go along a typical acoustic length (usually measured in meters) of the apparatus is of the same order as the time taken for a diffusion-type disturbance to travel a flame thickness (a few characteristic diffusion distances would be measured in millimeters at the most). The resonance obtained is usually associated with fluctuating heat loss and its effect on the acoustic perturbation in the velocity field either side of the flame and anchor point.[14,15] A velocity transfer function is derived that depends on flame parameters (such as Lewis number, heat release, and activation energy) and also initial standoff distance and frequency of oscillation. From this can be derived the change in acoustic impedance for the flame–gauze system and predictions made as to whether harmonic disturbances will grow or decay.[10] The outcome of this analysis is a velocity transfer function that has been used successfully to model real burner systems.[16] For these type of disturbances, the actual level of pressure disturbance is very small, but the effect is large: for a pressure oscillation with amplitude of only 2 Pa (2×10^{-5} of an atmosphere), the noise output is of the order of 100 dB.

For harmonic disturbances where the amplitude δ is of the order of θ^{-1}, then the analysis[9] at this length scale ($N \approx M^{-1}: \tau \approx 1$) indicates that as the frequency of oscillation ω_i goes up, so also the amplitude ratio of the burning rate compared with the pressure oscillation increases as $\sqrt{\omega_i}/2$, which indicates that shorter length scale disturbances cause the burning rate to be more sensitive. (Note that this is a transient phenomenon and not linked directly to the static dependence of mass burning rate on atmospheric pressure.)

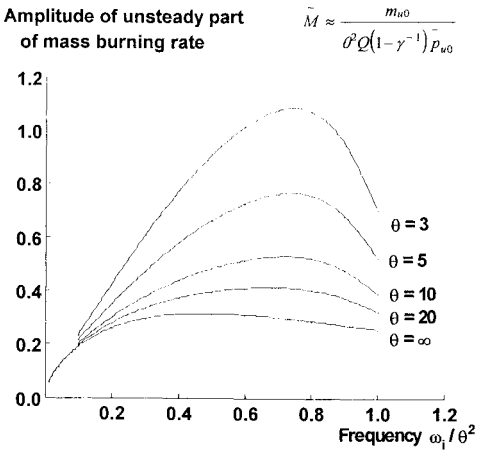

Fig. 3 Variation of amplitude of mass burning rate ratio $\bar{M}$ with frequency ω_i/θ^2 and activation energy θ (from Ref. 18).

This growth with frequency of the burning rate amplitude of oscillation reaches a peak at the smaller length scale $N \approx 1/(\theta^2 M): \tau \approx \theta^2$. For these shorter length scale disturbances the typical acoustic length is still much greater than a diffusion length, and so spatial pressure gradients are still not "felt" within the reaction zone. However, the acoustic time scale is now shorter than a typical diffusion time of the preheat zone and more in line with the typical reaction time. Consequently, an unsteady reaction zone emerges[17] at this balance of time scales, and there is effectively a reaction zone resonance at a specific frequency.

Thus the $\sqrt{\omega_i}/2$ behavior does not continue indefinitely, and there is a well-defined peak frequency (see Fig. 3).

The crucial point to note here is that the amplitude ratio is now measured in essentially units of θ^2. Thus for an activation energy θ of 10 the mass burning rate perturbation $\bar{m}_{u0}$ is 100 times as sensitive as the pressure perturbation $\bar{p}_{u0}$ (see Ref. 18). The ratio $\bar{M}$ defined as

$$\bar{M} \equiv \frac{1}{\theta^2}\left[\frac{\bar{M}_{u0}}{(1-\gamma^{-1})p_{u0}}\right]$$

is a useful way of presenting the data (Fig. 3), but in reality the more relevant and practical ratio is

$$\text{Linearized unsteady part of mass burning rate} \equiv \left[\frac{\bar{M}_{u0}}{(1-\gamma^{-1})p_{u0}}\right].$$

This is θ^2 times the appropriate curve in Fig. 3, so that there is a very great sensitivity to activation energy in the burning rate response that

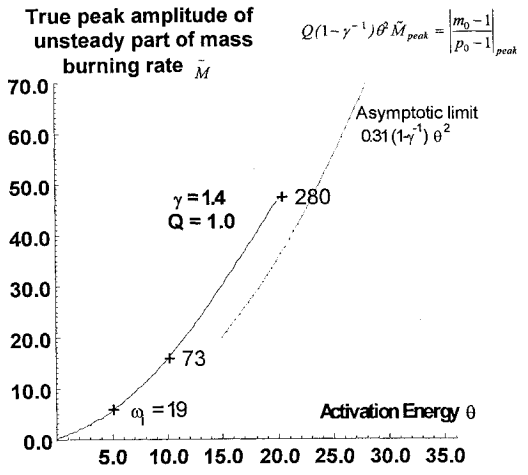

Fig. 4 Harmonic oscillations of burning rate. True variation of the peak of unsteady fluctuations plotted against activation energy θ. Peak frequency ω_f is also marked (from Ref. 18).

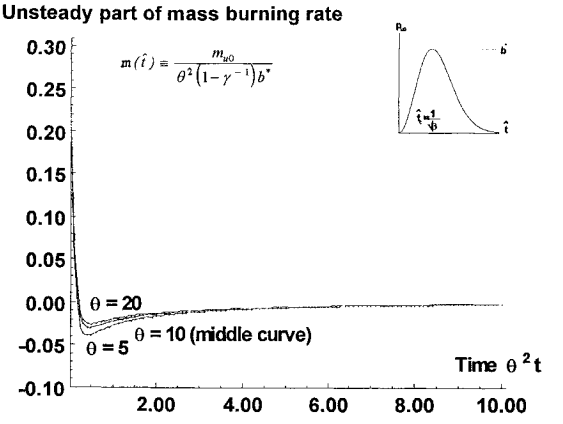

Fig. 5 Response of mass burning rate to a smooth pulse pressure input on the fast time scale. Time scale factor $\beta = 7$, hence peak pressure time $\hat{t}_c = 0.37796$ (from Ref. 18).

is somewhat hidden in these plots but brought out in Fig. 4 where the burning rate peak is plotted against activation energy θ.

Marked on this plot is the corresponding frequency where the peak occurs. In general terms, high activation energy means that the mass burning rate fluctuations are larger and faster.

One can, of course, increase the frequency further so that we are in the ultrahigh frequency wave region[19] [$\tau \approx M^{-1}(N \approx 1)$]. Such small length scale interactions would imply that acoustic waves are within the preheat zone, and it has been shown that, for sufficiently large amplitude ($\delta \approx \theta^{-1}$), nonlinearities develop that are much affected by the sharp density changes through the flame. Even at small amplitudes, there is quite a marked effect on an incoming acoustic wave[20] due in part to the effect of the flame on the jump conditions in pressure and velocity across the reaction zone.

B. Nonharmonic Inputs

Nonharmonic (but still one-dimensional) interactions have also been considered[9,18,21] that clearly indicate great sensitivity on the part of the burning rate to the rate of change of pressure.

For a linear decrease in pressure, there is a $\sqrt{t}$ dependence of the mass burning rate. The burning rate responds more quickly than the pressure change and is related more to the rate of change of pressure with time. This is why it is *rate* of deposition of energy in the initial explosion that is all important. The subsequent increase in mass burning rate from normal deflagration propagation levels is known from experimental evidence and disasters like Flixborough to be very much connected with the *time scale* of energy deposition.[1]

For a linear decrease in pressure at the $\tau \approx 1$ time scale, of the form

$$p_0 = 1 - \frac{t}{(1-\gamma^{-1})\nu\theta(1-Q)}$$

where Q is the heat release. Ledder and Kapila[21] have shown that the mass burning rate M reduces as $\sqrt{t}$:

$$M \approx 1 - \frac{1}{(1-Q)\nu}\sqrt{\frac{t}{\pi}}$$

with the prediction of flame extinction

$$\hat{t}_{ext} \approx (1-Q)^2\nu^2\pi$$

The effect of a pressure pulse can be to initially increase the mass burning rate. However, the *subsequent* behavior (*after* the initial pressure rise) is for the mass burning rate to undershoot its original value. Thus wild oscillations in the mass burning rate can be envisaged in a real situation with many pressure pulses going through an initially steadily propagating deflagration in its very early time history (i.e., less than 1×10^{-3} s).

A similar type of behavior is predicted for smaller length scale pressure disturbances [$N \approx 1/(\theta^2 M)$] such that the $\tau \approx \theta^2$ time scale causes the reaction zone to be near its natural response time.

Figure 5 shows the response to a smooth pulse input (of the form $2^{-\beta\hat{t}^2} - 2^{-2\beta\hat{t}^2}$) similar to that used by Ledder and Kapila[21] but at the faster time scale $\hat{t} = \theta^2 t$.

What is evident is that at very early times the response is exceedingly large (since the actual response is θ^2 times the $m(\hat{t})$ plotted in Fig. 5). Thus, although the later time history follows the trends of the $\tau \approx 1$ analysis (as one would expect), at very early times, the mass burning rate shoots up to exceedingly high values. To bear this out, we denote by δ a small parameter describing the level of input pressure disturbance and form the pressure and mass flux perturbation as follows:

$$p_0 = 1 + \delta p_{u0} = \left[1 + \delta\frac{p_{u0}^{(1)}}{\theta}\right]$$

$$m_0 = 1 + \delta m_{u0} = \left\{1 + \delta\left[\theta m_{u0}^{(0)} + m_{u0}^{(1)} + \cdots\right]\right\}$$

Thus for Fig. 5 the full response for the burning rate is

$$m_0 = 1 + \delta\theta^2(1-\gamma^{-1})b^* m$$

where

$$p_0 = 1 + \delta \cdot 4b^*\left(2^{-\beta\hat{t}^2} - 2^{-2\beta\hat{t}^2}\right)$$

and m is the burning rate function plotted in Fig. 5. The peak value of the pressure peak is then

$$p_{0\max} = 1 + \delta b^*$$

so that the full burning rate m_0 can be written as

$$m_0 = 1 + \theta^2(1-\gamma^{-1})(p_{0\max} - 1)m$$

For $\theta = 10$ and $\gamma = 1.4$, the value of the initial peak is approximately

$$m_{0peak} \approx 1 + 7.5(p_{0\max} - 1)m$$

Thus, although this is really only a linear theory, there is a strong indication that even for 0.5 bar peak overpressures, one can expect in the very early stages as much as a $2 \rightarrow 3$ transient increase of burning rate in the very early stages of a steep pressure wave interaction with a flame (this is apart from any two-dimensional effects).

Again we stress that this is the very early time history ($t \sim 10^{-5}$ s) where the burning has started but the pressure rise after ignition is so steep as to give a very abnormal transient growth in the burning rate.

These effects have been substantiated by a numerical code that has enabled ultrashort length scale interactions ($N \approx 1: \tau \approx M^{-1}$)

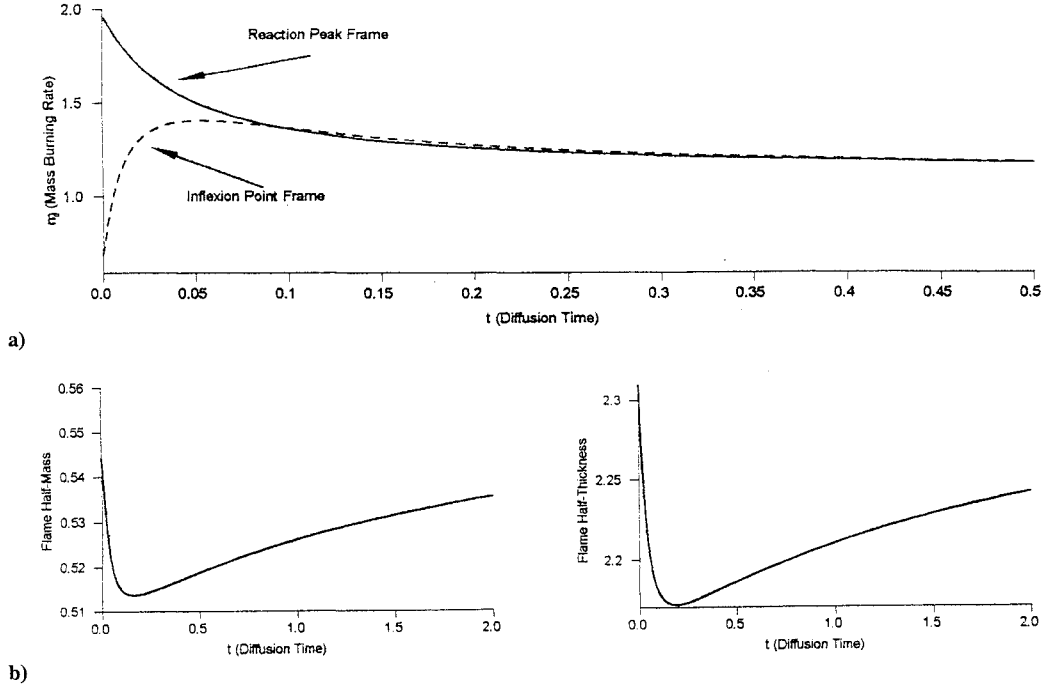

Fig. 6 One-dimensional interaction between a steep pressure pulse and a premixed flame of simple one-step chemistry (from Ref. 23). The first plot shows the local mass burning rate at two locations in the flame: a) the temperature inflexion point and b) the reaction rate peak. The second plot shows the change in the mass between these two locations, and the third plot indicates the change in the thickness of the flame (the distance between the two locations where the reaction rate $Ce^{-\theta/T}$ is at one-half its peak value). Pressure step 0.1 bar, activation energy $\theta = 10$, and ratio of unburnt to burnt temperature $T_{01} = 0.2$.

to be followed. The results of this work are reported on in recent work.[22,23] Not only is the trend of Fig. 5 confirmed by this work (see Fig. 6), but it can be seen that if the pressure wave is sufficiently steep, the mass burning rate is markedly different at different locations in the flame for the very beginning of the response (before a typical unit of combustion time has elapsed, i.e., $t \sim 10^{-7}$–10^{-5} s). Shown in Fig. 6 is the response at two locations in the flame defined by 1) where the point of inflexion is for the temperature profile and 2) where the maximum reaction rate occurs.

Thus when an ultra-short length scale pressure disturbance (close to a typical shock thickness) goes through a premixed flame, there are effectively two stages: first the effect *by the flame* on the pressure wave transmitted through and reflected by the combustion zone,[22] and then the effect *on the flame* after the blast wave has gone through and substantially altered the temperature field surrounding the deflagration.[23] Figure 6 is from the second reference and shows that at this time scale ($t \sim 10^{-6}$–10^{-5} s) different parts of the flame respond with different burning rates so that the reaction zone broadens or contracts as it finds a new equilibrium. The example shows the response for an instantaneous shock of 0.1 bar to a flame with activation energy $\theta = 10$ and temperature ratio unburnt to burnt $T_{01} = 0.2$. Very evident is the "squeezing" of the combustion region between the inflexion point and reaction peak locations due to the very different values of the local mass burning rate at these points. Thus there is a transient expulsion of gas between these two locations. Very large (but momentary) changes in overall burning rate can therefore take place even for what may appear to be simple one-dimensional flame/pressure wave interactions.

IV. Two-Dimensional Interactions

A. Enhancement of the Wrinkling of Flames Due to the Rayleigh–Taylor Instability

Figure 7 is a schematic of the Rayleigh–Taylor instability. In our case the acceleration due to gravity is replaced by the pressure gradient. From the momentum equation $-\nabla p/\rho$ will have an equivalent effect in accelerating the fluid by different amounts because of the disparity in density between the hot and cold gases. Such an effect has been observed by Tsuruda and Hirano.[24] This

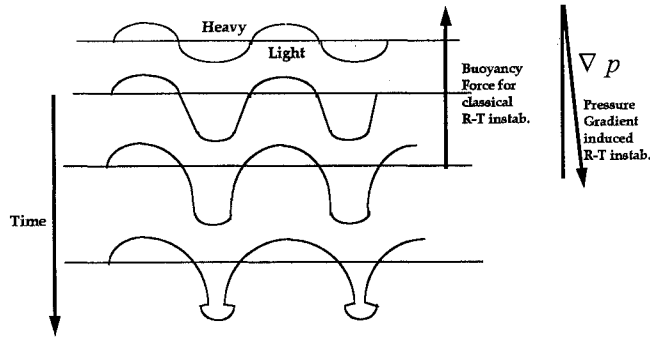

Fig. 7 Schematic of the Rayleigh–Taylor instability applied to premixed flames.

reference includes photographs, the essence of which have been reproduced by a numerical approach that treats the flame as a discontinuity.[25]

If a linear gradient in pressure is introduced from the burnt (light density) side, then this induces (by differential acceleration) a larger velocity near the peak than the trough. This then causes a spike to develop such that a "tongue" of unburnt reactants is pushed into the hot (burnt) products. One should recognize that the overall progress of the wrinkled premixed flame in units of combustion time ($\sim 10^{-3}$ s) is still in the direction of the heavy (unburnt) gases, but that during the passage time of the pressure wave ($\sim 10^{-8}$ s) significant relative velocities are induced in the other direction (heavy to light) due to differences in the effect of the imposed pressure gradient. The differences in density at different lateral locations encountered by the planar pressure wave lead to differential induced velocities. If the pressure gradient is in the other direction [that is where the pressure gradient is introduced from the cold (heavy) side], then the instability is suppressed.[25] Initially the same spikes are found in numerical models that use a distributed reaction zone. However, it is only with the more realistic model of the reaction that one can properly simulate the spherical lobes of unburnt gas that form at the end of the spikes entering the lighter fluid. These investigations[26] show that, after the initial stage, a Kelvin–Helmoltz type instability is observed due to the shear flow of the heavy spike of fluid against

the light fluid surrounding it. This creates a secondary vortex system leading to the lobes of unburnt gas at the end of the initial unburnt protrusion into the hot products. The subsequent development of the flame will be much affected by the increased burning rate, which is encouraged by the greater heat transfer from hot products to cold reactants. This instability will enhance the turbulent breakup of a laminar flame and so further increase the mass burning rate because of the increase in the flame area. When this is combined with the one-dimensional effects already mentioned for increasing the local mass burning rate of individual flamelets, there is an overall strong mechanism for acceleration from low deflagration speeds (on the order of 0.1–0.5 ms^{-1}) to values that are still subsonic but large (100–200 ms^{-1}).

B. Breakup of Flames Due to Strong Vorticity—the Baroclinic Effect

If the premixed flame is strongly curved already and the pressure disturbance is sharp, then the $\nabla\rho \wedge \nabla p$ term in the vorticity generation equation,

$$\frac{D(\underline{\omega}/\rho)}{Dt} = \frac{\nabla\rho \wedge \nabla p}{\rho^3} + \left(\frac{\underline{\underline{\omega}}}{\rho} \cdot \nabla\right)\underline{u} + \nu\nabla^2\left(\frac{\underline{\underline{\omega}}}{\rho}\right)$$

induces strong roll-up of the flame surface. This effect is simply a more accentuated form of the Rayleigh–Taylor instability and is highly relevant to the large acceleration observed in the flame propagation rate in vented explosions when the flame front reaches the region of the vent.[27,28]

As indicated in Fig. 8 there is a pressure gradient due to a decompression wave in a vented explosion that is operating in the unstable direction for the Rayleigh–Taylor instability. If the expansion wave is severe, then the vorticity production can be such as to break up the flame into a turbulent flame brush. Figure 9 illustrates the curling up of a spherical flame by the impact of a shock wave.

A numerical method for solving the two-dimensional reactive Navier–Stokes equations has been successfully developed by Falle[29] and is used here to simulate the interaction of a shock wave with a flame ball[30] (the situation shown schematically in Fig. 9). Figure 10 indicates the density contours of the flame after the shock wave has passed through, clearly showing the generation of a strong vortex

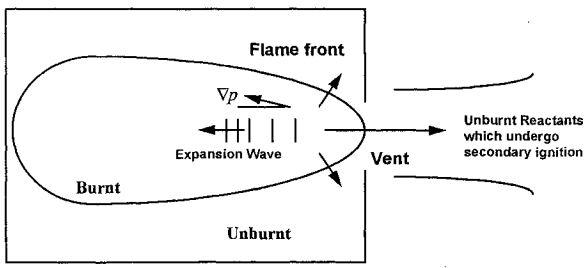

Fig. 8 Schematic of vented explosion showing the flame front near a vent and decompression wave passing through.

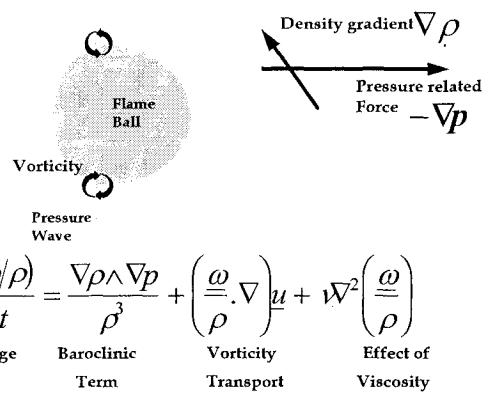

Fig. 9 Baroclinic generation of vorticity due to a shock wave passing through a curved flame.

field that eventually breaks up the flame into two. This is effectively a numerical version of the experiment done by Markstein.[31]

V. Discussion

A. Main Effects of Pressure Waves Interacting with Initial Flame Kernel

From the preceding outline of the major results of pressure interactions with laminar premixed flames, it is apparent that there can be many types of pressure wave interactions that may drastically alter the progress of a flame front after an explosion.

Consider the scenario of a large leakage of flammable gas in a region that is partially confined, with subsequent ignition taking place. Immediately after ignition, a combustion wave is sent out that initially (within the first 10^{-7} to 10^{-8} s) travels at a slow speed (less than 1 ms^{-1}). After this, the progress of the flame is affected by a variety of factors that contribute to the rapid acceleration of the combustion front.

The consequent expansion of hot gases sends a compression wave ahead of the flame front, which can lead to a number of effects. The following are the most significant.

1) Transient local changes in burning rate: If there is some confinement and/or obstacles are present, then the initial pressure wave from the first ignition can be reflected back through the deflagration front, which will invoke transient (one-dimensional) accelerative mechanisms for the burning rate due to severe distortion of the reaction zone.

2) Increases in flame surface area due to the Rayleigh–Taylor instability: If the flame front is curved, then even long length scale pressure disturbances will bring about severe distortion of the flame front.[24–26] This increases the flame surface area and so provides a large increase in the overall burning rate. This can be particularly relevant in vented explosions where a strong decompression wave can invoke rapid changes leading to a turbulent flame structure.

3) Baroclinic break-up of flame by vorticity: For sharp, large-amplitude pressure wave interactions, the vorticity generation by the baroclinic effect is so strong as to break up the flame into a turbulent flame brush. This is due to the pressure gradient being inclined to the density gradient, leading to a component of force at right angles to the main direction of flow, thus provoking the gases to swirl. This provides a much greater mixing of the cold reactants in the vicinity of hot products and so provides a third mechanism for the increase in the burning rate of the mixture.

4) Preheating: For a strong shock there can be substantial preheating of the cold reactants that can again speed up the overall burning rate. This is particularly relevant if there is considerable turbulence in the mixture to begin with. Although we have at present only considered laminar theories, by regarding the flame as a series of laminar flamelets,[32] with a correspondingly larger initial overall (turbulent) flame speed, for sufficiently strong shocks, one may get a further ignition event ahead of the first flame front. This then leads to further pressure disturbances emitted ahead and also back to the first deflagration zone (providing a feedback mechanism).

5) Persistent acceleration—the onset of a detonation: The effect of all of the preceding four mechanisms can be to so accelerate the flame that it generates its own compression wave ahead of itself (this is apart from the initial compression wave associated with the ignition event). Another feedback mechanism can now be set up whereby pressure waves are sent out ahead of the flame and reflected from obstacles and boundaries back through the flame, which consequently further enhance the growth in flame speed. Hence further compression waves are emitted ahead of the combustion front, so that a snowball effect develops, which can result in the flame catching up with the compression waves. This process is effectively the onset of a detonation wave.

All of these mechanisms are therefore inextricably linked together and encourage a strong feedback mechanism into the overall burning rate.

Evidently if the ignition event takes place over a longer time scale, and the energy emitted to the gases can dissipate more slowly, then the consequent pressure wave is that much weaker and some of the aforementioned mechanisms will not be very important. The

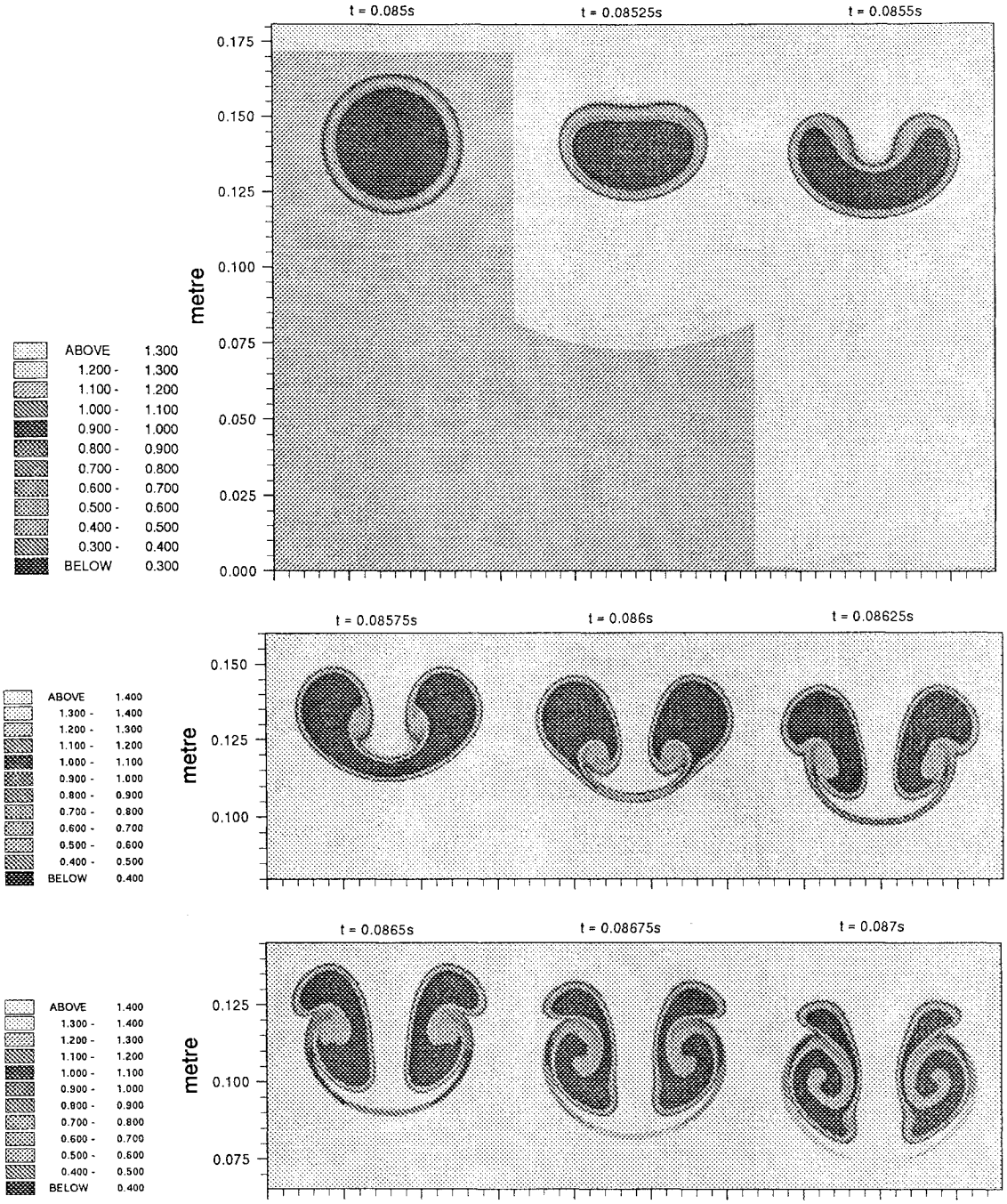

Fig. 10 The effect of a shock wave of strength 0.3 bar propagating across a flame ball with local laminar flame speed 7.75 ms^{-1}. Upstream temperature 300 K and downstream temperature 1500 K. Reaction rate constant $k_0 = 5 \times 10^{-7}\ s^{-1}$. Reaction rate = $k_0 C e^{-\theta/T}$, with $\theta = 10$. Thermal conductivity $\lambda \alpha T$ with λ (300 K) = 0.1 $Jm^{-1}\ s^{-1}\ K^{-1}$. Upstream density ρ (300 K) = 1.17 $kg\,m^{-3}$ and thermal diffusivity K (300 K) = $9 \times 10^{-5}\ m^2\ s^{-1}$. Lewis no. $Le = 1$ and Schmidt no. $Sc = 1$. The plots of density contours show the effect of baroclinicity in generating a strong vortex field, which eventually causes the flame ball to split into two. (From Ref. 30.)

important factor is the *rate* of pressure rise in the very first stages of ignition. This is a function of how sharply the initial ignition event takes place.

B. Calculations of the Increase in Overall Burning Velocity as a Result of Pressure Interactions

From the work presented in this paper, the one-dimensional effects alone can lead to (typically) a local, but transient, threefold increase in the burning velocity (see Sec. III.B). What now follows is an estimate as to the increase in surface area obtained by first having a rippled (cellular) flame, the cells of which are the accentuated by the Rayleigh–Taylor effect.

Consider a flame surface initially flat that then becomes a sinusoidal flame surface with characteristic cell size c'. If the height of the sinusoidal surface is a', then the equation of the surface is given by

$$z' = a' \sin\left(\frac{\pi x'}{c'}\right) \sin\left(\frac{\pi y'}{c'}\right)$$

The increase in surface area for a given height a' in cartesian coordinates is given by

$$S' = \int_0^{c'}\int_0^{c'} \mathrm{d}S'$$

$$= \int_0^{c'}\int_0^{c'} \sqrt{1 + \left(\frac{\partial z'}{\partial x'}\right)^2}\sqrt{1 + \left(\frac{\partial z'}{\partial y'}\right)^2}\,\mathrm{d}x'\,\mathrm{d}y'$$

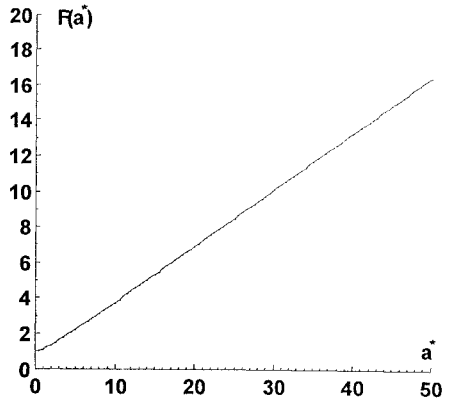

Fig. 11 Fractional increase F in surface area of a sinusoidal three-dimensional surface as a function of normalized height a^*.

where $dS' = ds'_1\, ds'_2$ is considered as the multiplication of two arc lengths ds'_1 and ds'_2. Thus

$$S' = \int_0^{c'}\int_0^{c'} \left[1 + \left(\frac{\pi a'}{c'}\right)^2 \cos^2\left(\frac{\pi x'}{c'}\right) \sin^2\left(\frac{\pi y'}{c'}\right)\right]^{\frac{1}{2}} \times \left[1 + \left(\frac{\pi a'}{c'}\right)^2 \sin^2\left(\frac{\pi x'}{c'}\right) \cos^2\left(\frac{\pi y'}{c'}\right)\right]^{\frac{1}{2}} dx'\, dy'$$

i.e., $S' = c'^2 F(a^*)$ where

$$F(a^*) \equiv \frac{1}{\pi^2}\int_0^{\pi}\int_0^{\pi} [1 + (a^*)^2 \cos^2(x^*) \sin^2(y^*)]^{\frac{1}{2}} \times [1 + (a^*)^2 \sin^2(x^*) \cos^2(y^*)]^{\frac{1}{2}}\, dx^*\, dy^*$$

and $a^* \equiv \pi a'/c'$, $x^* \equiv \pi x'/c'$, and $y^* \equiv \pi y'/c'$.

This function $F(a^*)$ can easily be worked out numerically and is plotted in Fig. 11.

For perturbed flame fronts with typical cell sizes of about 3–4 $\times 10^{-3}$ m, with a ripple height of 1×10^{-3} m, then a^* is in the region of $0.75 \rightarrow 1$. This leads to a small increase in surface area ($F \approx 1.1$) for the cellular flame. Thus if the mixture has a typical burning velocity of 0.3 ms^{-1}, then after a transient increase to approximately 0.9 ms^{-1} due to the passage of the pressure wave, any small-scale rippling of the flame will only slightly increase the burning velocity to a value on the order of 1 ms^{-1}.

Now consider the Rayleigh–Taylor effect on this rippled flame and the consequent increase in surface area. Typically the depth of the cells can increase to values of the order of $2 \rightarrow 3 \times 10^{-2}$ m in a very short space of time (less than 1×10^{-3} s). This corresponds to a value of a^* in the region of 30 and a fractional increase F in the area of about 10. Undoubtedly locally the burning velocity will no longer be in the z' direction, and it is known that this is altered by flame stretch with an appropriate Markstein number. However, apart from local flame extinction (which is not considered here), the overall mass burning rate for a distorted laminar flame will increase in proportion to the increase in flame surface area. Thus in this simple calculation we take the overall burning velocity as being the mass burning rate divided by upstream density ρ' and the original cross-sectional area A' occupied by a flat flame, i.e.,

Average burning velocity:

$$\bar{u}' = (M'/\rho' A')$$

Thus, if the increase in surface area due to the Rayleigh–Taylor effect occurs at a time coincident with a rapid increase in burning velocity due to the (one-dimensional) distortion of the reaction zone, a further tenfold increase in overall burning velocity with values in the region of 10 ms^{-1} is predicted. At these speeds the flame will begin to set up its own compression waves, which upon reflection from obstacles can invoke the baroclinic distortion of the flame into a turbulent flame brush. So it can be seen that these early stages of the explosion are crucial in the later acceleration of the combustion processes.

VI. Conclusions

The preceding studies show that, whether by shock ignition or pressure wave reflection, the interaction of pressure waves with an existing flame front is crucial in the early stages of explosion development. It is evident that pressure effects within the first 10^{-3} s or so after ignition can be very important in accelerating the overall turbulent flame brush. These initial events happen on an *acoustic* scale (10^{-7}–10^{-5} s) but can be exceedingly important in understanding the subsequent progress of the explosion.

References

[1]Gugan, K., "Unconfined Vapour Cloud Explosions," Institute of Chemical Engineers and Godwin Ltd., London, 1979.

[2]Cullen, W. D., Lord, "The Public Inquiry into the Piper Alpha Disaster," Vols. 1 and 2, Dept. of Energy, HMSO, London, 1991.

[3]Lee, J. H. S., "On the Transition from Deflagration to Detonation," *Dynamics of Explosions*, edited by J.R. Bowen, J. C. Leyer, and R. I. Soloukhin, Vol. 106, Progress in Astronautics and Aeronautics, AIAA, New York, 1986, pp. 3–11.

[4]Lee, J. H. S., and Moen, I. O., "The Mechanism of Transition from Deflagration to Detonation in Vapour Cloud Explosions," *Progress in Energy and Combustion Science*, Vol. 6, 1980, pp. 359–389.

[5]Moen, I. O., Donato, M., Knystautas, R., and Lee, J. H., "Flame Acceleration Due to Turbulence Produced by Obstacles," *Combustion and Flame*, Vol. 39, 1980, pp. 21–32.

[6]Oppenheim, A. K., Lundstrom, E. A., Kuhl, A. L., and Kamel, M. M., "A Systematic Exposition of the Conservation Equations for Blast Waves," *Journal of Applied Mechanics*, Vol. 38, 1971, pp. 783–794.

[7]Guirguis, R. H., Oppenheim, A. K., and Kamel, M. M., "Self-Similar Blast Waves Supported by Variable Energy Deposition in the Flowfield," *Gas Dynamics of Detonations and Explosions*, edited by J. R. Bowen, N. Manson, A. Oppenheim, and R. I. Soloukhin, Vol. 75, Progress in Astronautics and Aeronautics, AIAA, New York, 1981, pp. 178–192.

[8]Oran, E. S., and Gardner, J. H., "Chemical-Acoustic Interactions in Combustion Systems," *Progress in Energy and Combustion Science*, Vol. 11, 1985, pp. 253–276.

[9]McIntosh, A. C., "Pressure Disturbances of Different Lengthscales Interacting with Conventional Flames," *Combustion Science Technology*, Vol. 75, 1991, pp. 287–309.

[10]McIntosh, A. C., "Flame Resonance and Acoustics in the Presence of Heat Loss," *Lectures in Applied Maths*, Vol. 24, Part 1, American Mathematical Society, Providence, RI, 1986, pp. 269–301.

[11]McIntosh, A. C., "The Effect of Upstream Acoustic Forcing and Feedback on the Stability and Resonance Behaviour of Anchored Flames," *Combustion Science and Technology*, Vol. 49, 1986, pp. 143–167.

[12]McIntosh, A. C., "Combustion-Acoustic Interaction of a Flat Flame Burner System Enclosed Within an Open Tube," *Combustion Science and Technology*, Vol. 54, 1987, pp. 217–236.

[13]Van Harten, A., Kapila, A. K., and Matkowsky, B. J., "Acoustic Coupling of Flames," *SIAM Journal on Applied Mathematics*, Vol. 44, No. 5, 1984, pp. 982–995.

[14]McIntosh, A. C., "On Flame Resonance in Tubes," *Combustion Science and Technology*, Vol. 69, 1990, pp. 147–152.

[15]McIntosh, A. C., "Some Comments on the Rayleigh Criterion for Combustion-Associated Acoustic Resonance," *Proceedings of the Joint Meeting of the British and German Sections of the Combustion Institute (Cambridge)*, edited by K. N. C. Bray et al., Combustion Inst. (UK), 1993, pp. 323–326.

[16]Raun, R. L., and Beckstead, M. W., "A Numerical Model for Temperature Gradient and Particle Effects on Rijke Burner Oscillations," *Combustion and Flame*, Vol. 94, 1993, pp. 1–24.

[17]Stewart, D. S., "On the Stability of the Reaction Zone of the Plane Deflagration," *Combustion and Flame*, Vol. 64, 1986, pp. 157–165.

[18]McIntosh, A. C., "The Linearised Response of the Mass Burning Rate of a Premixed Flame to Rapid Pressure Changes," *Combustion Science and Technology*, Vol. 91, Nos. 4–6, 1993, pp. 329–346.

[19]McIntosh, A. C., "The Interaction of High Frequency, Low Amplitude Acoustic Waves with Premixed Flames," *Non Linear Waves in Active Media*, edited by J. Engelbrecht, Springer–Verlag, Heidelberg, Germany, 1989, pp. 218–231 (*Proceedings of Euromech* 241, Tallinn, Estonia, Sept. 1988).

[20]McIntosh, A. C., and Wilce, S. A., "High Frequency Pressure Wave Interaction with Premixed Flames," *Combustion Science and Technology*, Vol. 79, 1991, pp. 141–155.

[21]Ledder, G., and Kapila, A. K., "The Response of Premixed Flames to Pressure Perturbations," *Combustion Science and Technology*, Vol. 76, 1991, pp. 21–44.

[22]McIntosh, A. C., Batley, G., and Brindley, J., "Short Lengthscale Pressure Pulse Interactions With Premixed Flames," *Combustion Science and Technology*, Vol. 91, Nos. 1–3, 1993, pp. 1–13.

[23]Batley, G., McIntosh, A. C., and Brindley, J., "The Time Evolution of Interactions Between Short Lengthscale Pressure Disturbances and Premixed Flames," *Combustion Science and Technology*, Vol. 92, Nos. 4–6, 1993, pp. 367–388.

[24]Tsuruda, T., and Hirano, T., "Local Flame Disturbance Development Under Acceleration," *Combustion and Flame*, Vol. 84, 1991, pp. 66–72.

[25]Liu, F., McIntosh, A. C., and Brindley, J., "A Numerical Investigation of Rayleigh-Taylor Effects in Pressure Wave-Premixed Flame Interactions," *Combustion Science and Technology*, Vol. 91, Nos. 4–6, 1993, pp. 373–386.

[26]Edwards, N. R., McIntosh, A. C., and Brindley, J., "The Development of Pressure Induced Instabilities in Premixed Flames," *Combustion Science and Technolgy*, Vol. 99, Nos. 1–3, 1994, pp. 179–200.

[27]Van Wingerden, C. J. M., and Zeeuwen, J. P., "On the Role of Acoustically Driven Flame Instabilities in Vented Gas Explosions and Their Elimination," *Combustion and Flame*, Vol. 51, 1983, pp. 109–111.

[28]Cooper, M. G., Fairweather, M., and Tite, J. P., "On the Mechanisms of Pressure Generation in Vented Explosions," *Combustion and Flame*, Vol. 65, 1986, pp. 1–14.

[29]Falle, S. A. E. G., "Self-Similar Jets," *Monthly Notices of the Royal Astronomical Society*, Vol. 250, 1991, pp. 581–596.

[30]Batley, G. A., McIntosh, A. C., Brindley, J., and Falle, S. A. E. G., "A Numerical Study of the Vorticity Field Generated by the Baroclinic Effect due to the Propagation of a Planar Pressure Wave Through Cylindrical Premixed Laminar Flame," *Journal of Fluid Mechanics*, Vol. 279, pp. 217–237, 1994.

[31]Markstein, G. H., *Non-Steady Flame Propagation*, AGARDograph 75, Pergamon, Oxford, England, UK, 1964.

[32]Bray, K. N. C., Libby, P. A., Masuya, G., and Moss, J. B., "Turbulence Production in Premixed Turbulent Flames," *Combustion Science and Technology*, Vol. 25, 1981, pp. 127–140.